EARTH'S CRYOSPHERE
SCIENTIFIC JOURNAL

Earth`s Cryosphere, 2017, vol. XXI, No. 6, pp. 39–47 **http://earthcryosphere.ru/**

ICE AND FROZEN GROUND PROPERTIES

DOI: 10.21782/EC1560-7496-2017-6(39-47)

THE SEARCH FOR FERROELECTRIC ICE IN POROUS MEDIA ON THE EARTH

G.S. Bordonskiy, A.O. Orlov

Institute of Natural Resources, Ecology and Cryology, SB RAS,
16a, Nedorezova str., Chita, 672014, Russia; lgc255@mail.ru

In search of ferroelectric ice, the thermal measurements of wet nanoporous silicates when cooled down to –150 °C and experiments on measuring own low-frequency electric fluctuations, dielectric parameters at low frequencies and microwaves have been carried out. The findings have been interpreted as formation the ferroelectric ice 0 in supercooled pore water at temperatures below –20 °C. The existence of ice XI on the Earth remains an open issue.

Supercooled water, nanoporous silicates, ferroelectric properties, ice 0, ice XI

INTRODUCTION

It is currently believed that at atmospheric pressure and at temperatures which may occur in terrestrial conditions, two crystal modifications of ice, Ih and Ic may exist [*Kirov, 1996; Chaplin, 2016*]. In addition, it was stated in [*Fukazawa et al., 1998*] that in Antarctica ferroelectric ice XI was formed when protons were ordered in ice Ih at the temperature –36 °C. However, it takes 10^2–10^4 years for it to be formed. This statement remains debatable, as the study conducted in [*Fortes et al., 2004*] on Antarctic ice aged 3000 years did not confirm the presence of a registered amount of ice XI. Therefore, it is considered that in terrestrial conditions, ice XI is absent, and experiments demonstrate a narrow temperature range of its existence: 57–72 K. Yet, it should exist on the cold planets of the Solar system – Uranus, Neptune, Pluto, their satellites, comets, and asteroids [*Fukazawa et al., 2006*].

At the same time, it was shown in [*Arakawa et al., 2011*] that small domains of three-dimensional ice XI were present in common ice in the case of heating ice XI to the temperature 111 K (–162 °C). This phenomenon was named 'a memory effect'. This effect took place in heating ice XI, and this ice was transformed into ice Ih, whereas after subsequent cooling, ice XI was formed at a higher temperature. In [*Arakawa et al., 2011*] a conclusion was made based on the experimental results and the data provided by other authors that the domains of ice XI existed before the temperature of about 150 K (–120 °C). Due to their insignificant concentration, they are not registered by the methods of neutron diffraction and Raman scattering (the sensitivity of these methods is ~1 % of the total mass of a sample under study).

As atmospheric ice XI may exist at atmospheric pressure, a question arises, whether it may originate under natural conditions on the Earth in some special cases. Perhaps, water being in porous materials may be such a special case. Depending on the pore geometry, water in the pores may be close to one-dimensional structures (filaments composed of water molecules) and to two-dimensional formations with large surface, when surface effects begin to prevail. Indeed, water in porous materials may stay unfrozen until the temperature of –90 °C, if the pore size diminishes to ~1 nm [*Limmer and Chandler, 2012*]. In porous materials, along with the common hexagonal ice Ih, ice crystals of Ic [*Sliwinska-Bartkowiak et al., 2008*] were found. Interesting results were obtained in [*Jazdzewska et al., 2011*], in which the method of neutron diffraction was used, and heavy water (deuterium oxide) was investigated. Along with ice Ih and ice Ic, crystalline modifications of ice VIII и IX were discovered in nanoporous carbon. These modifications may exist only at high pressures; therefore, it was concluded that the capture of water into pores generated an effect equivalent to the rise of pressure. Its value is determined by the forces of molecular interaction in the ice layers adjacent to the pore walls.

In [*Pan et al., 2008*], surface energy and proton ordering of ice in volume and on the surface of crystals was investigated. It was stated that, as ice XI in the ordered state was heated to temperature ~72 K, the surface order of ice was not destroyed until the melting point was reached. This result was based on the experimental data of previous works. For example, in [*Su et al., 1998*] ferroelectric ice film was observed when water was condensed from vapor on the

surface of a platinum crystal cooled to –136 °C. It seems that in this case the surface effects prevailed over the volume effects. Ferroelectricity was discovered in a one-dimensional case, a supramolecular structure, into which quasi-one-dimensional chains were embedded $(H_2O)_{12n}$ [*Zhao et al., 2011*]. The authors of this work observed an anomalous rise in dielectric permittivity at 175 and 277 K due to transition to the ferroelectric state.

It is evident that one-dimensional, two-dimensional structures and structures of water molecules of a special shape may possess a wide range of electric properties. Such a complicated structure consisting of structures of transition from supercooled water to ice [*Russo et al., 2014*] was found by using molecular dynamics methods. The new modification of ice was named 'ice 0': it is formed from supercooled water, followed by the emergence of ice Ih or ice Ic. This ice does not have a certain position on the phase diagram and is a transitional form in freezing of water. According to the authors [*Russo et al., 2014*], ice 0 plays the major role in transition of liquid to the solid phase. However, so far, there is no experimental confirmation of its existence. It is assumed that the scenario of transition of liquid into a solid state with emergence of a precursor takes place in crystallization of some other substances, for example, of Si, Ge and C.

In [*Quigley et al., 2014*], other possible metastable transition forms of ice were investigated, together with ice 0. Ice 0 was found to be ferroelectric, with its melting temperature being approximately –23 °C. However, water is rarely supercooled to such temperature in nature (the lowest water temperature was observed in water drops in clouds to be –37.5 °C [*Rosenfeld and Woodley, 2000*]). Therefore, formation of ice 0 is most probable in the natural environment in porous bodies, the pore sizes of which are small and in which copercooling by dozens of degrees below 0 °C is reached.

The objective of this study was to carry out an experimental investigation of phase transitions of water in nanoporous media at the temperature conditions which may take place in the Earth's cryosphere, at which ferroelectric forms of ice are formed (ice XI and ice 0). Such forms are quite interesting in terms of cryochemical transformations in frozen disperse media due to the significant difference between the chemical potentials of inclusions of ferroelectric ice and of the common modification of ice Ih. The results of previously made measurements have been analyzed, and the data of new experiments have been provided.

DESCRIPTION OF THE EXPERIMENTS

Ferroelectric materials are known to have specific electric characteristics – the presence of an electric domain structure, the Curie point (the temperature of transition from the ferroelectric to paralectric state), higher values of dielectric permittivity and own electric fluctuations. These characteristics allow researchers investigating such media to use the technique of dielectric spectroscopy, registration of own electric fluctuations, impedance spectroscopy, acoustic electric measurements, and radiointroscopy. These methods have the advantage of being highly sensitive to a low fraction of the substance of ferroelectric inclusions in a paraelectric medium (which may be much less than 1 % of the total mass of a sample) in combination with the simplicity of the experimental setups used.

In this work, the method of measuring electric noise at low frequencies was used [*Musevic et al., 1997; Stukova et al., 2012*]. The use of low frequencies (less than 1 kHz) increases sensitivity of the method to phase transitions, which involve changes in the electric structure. This is due to the fact that in ferroelectric materials the Barkhausen effect occurs, related to polarization jumps when external parameters (electrical field, temperature, or pressure) change. The Barkhausen effect rises as the frequency goes down; therefore, in measuring the noise, the range section from 1 to 100 Hz was investigated.

In addition, the dielectric parameters of the media were measured: the real (ε′) and imaginary (ε″) parts of relative dielectric permittivity at the frequencies from 100 Hz to 100 kHz; their relation $\varepsilon''/\varepsilon' = \mathrm{tg}\,\delta$ was found, where tg δ is the loss tangent of the dielectric. The microwave parameters of the samples were investigated – attenuation of electromagnetic radiation and the reflection index by power from the flat air–medium borderline in a long waveguide. It was assumed in microwave measurements that phase transitions in a medium may form additional structures, for example, films having special properties on the borders between the water structures and the surface of the particles. Additional information was obtained by using differential thermal analysis, allowing detection of first-order phase transitions.

As noted above, in order to achieve significant supercooling of water, porous media with the nanometric size of pores may be used. In this case, a question arises regarding differences between the characteristics of porous and volume water. It was shown in [*Menshikov and Fedichev, 2011; Fedichev and Menshikov, 2013*] that for the pore size greater than 3 nm, the larger part of water is close to volume water for its characteristics. The layers from one to three water molecules thick have a structure determined by the pore material near the solid surface. The properties of volume water in nanopores are preserved until approximately its freezing point, which was established by the results of measuring attenuation of microwave emission in wetted silica gel with the average pore size 8 nm [*Bordonskiy and Krylov, 2012*]. It was shown in [*Castrillon et al., 2009; Fedichev and Menshikov,*

2012], in which the characteristics of water in nanoporous silicates were studied by the method of molecular dynamics, that the structure of water in such material approaches that of volume water at the distance of ~0.4 nm from the pore wall.

In the measurements, silicate materials were used – Acros silica gel used in chromatography, with the average pore diameter being 6 nm, and synthesized mesostructured material (SBA-15) with hexagonally ordered cylindrical pores 10.8 nm in diameter; there was a certain number of pores in the structure of the medium with the average diameter 2 nm and with the volume of about 10 % of the total volume. The phase transition for silica gel at water freezing took place at the temperature –20 °C, and for SBA-15, it occurred at –10 °C (for pores 10.8 nm in diameter) and –80 °C (for pores ~2 nm).

The melting point in the pores was evaluated by the formula

$$\Delta T = A/(r - \tau),$$

where ΔT is the decrease in the melting point compared to volume ice in empty space; $A = 52$ °C·nm; r – radius of a cylindrical pore, nm; $\tau = 0.38$ nm characterizes the thickness of a layer of strongly bound water [*Schreiber et al., 2001*]. Phase transitions in such media are vague and extended to the interval reaching 10 °C, with the phase transition point further decreasing when pores are not fully filled with water.

The measurement procedure. Electric noise measurement was conducted using a cylindrical cell with the internal diameter of 10 mm. On the cylinder bases, there were round metal electrodes, between which the powder material 2 cm^3 in volume was placed for study. The cell was switched to the amplifier input with a passband 1–100 Hz, with the voltage amplification factor being 10^3. The input resistance of the amplifier was 4.7 MOhm. The amplified signal was transmitted to the linear amplitude detector and the RC-filter of low frequencies with a unit constant 1 s. The cell was in a screened chamber to which cooling nitrogen vapor was fed at a constant feeding rate, using an electric vaporizer. The substance temperature was measured with a thermocouple. The relative calorimetric measurements were made by the derivative of temperature/time (dT/dt), which allowed us to determine the phase transition points with heat emission and absorption. The accuracy of the absolute temperature measurements was 0.2 °C. The sample cooling and heating rates remained uniform and constituted 1–2 °C/min. The data Agilent collection system was used. The dielectric measurements at the frequencies from 25 Hz to 1 MHz were made with a RCL gauge using a capacitive cell. A more detailed description of low-frequency electrical measurements is provided in [*Bordonskiy and Orlov, 2014*].

The lay-out of a microwave measurement setup is shown in Fig. 1. The microwave measurements con-

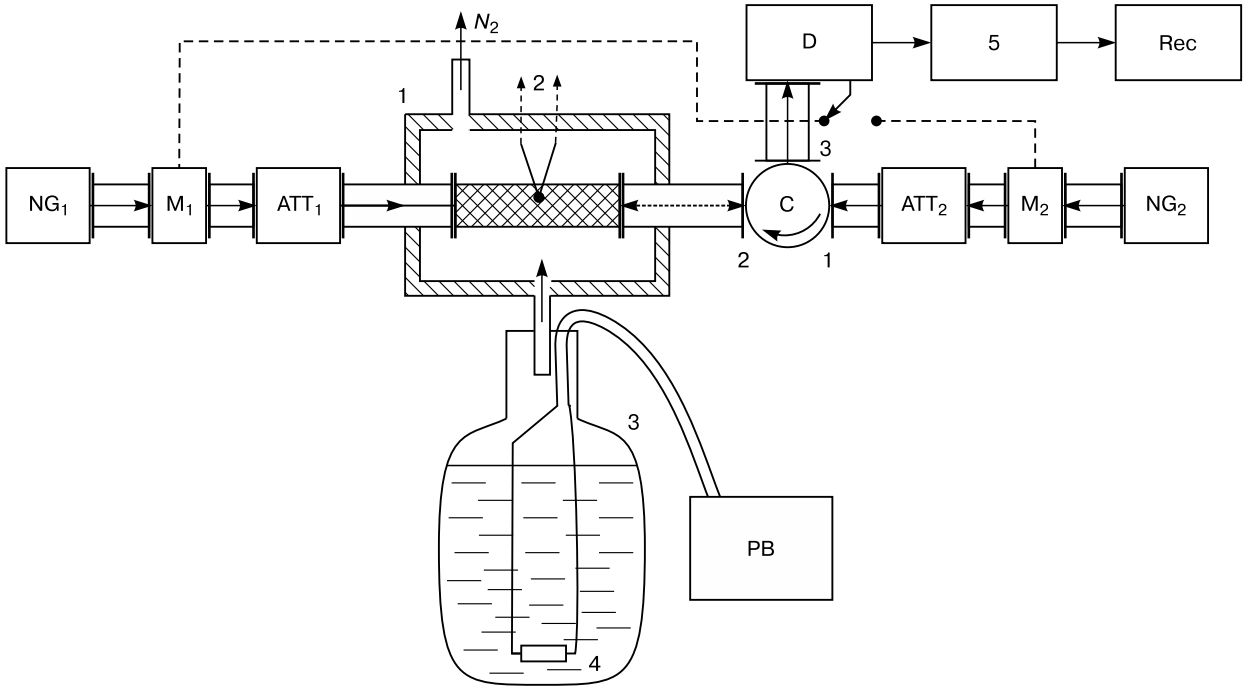

Fig. 1. A schematic of a measurement setup.

$NG_{1,2}$ – generators of microwave emission noise; $M_{1,2}$ – modulators; $ATT_{1,2}$ – attenuators for signal adjustment; C – three-port circulator; PB – power box for heating the resistor-evaporator; D – detector of microwave emission; Rec – recorder; 1 – thermal chamber with a sample placed into a waveguide, cooled with cold nitrogen vapor; 2 – thermocouple; 3 – Dewar vessel; 4 – resistor-evaporator; 5 – Agilent data collection system.

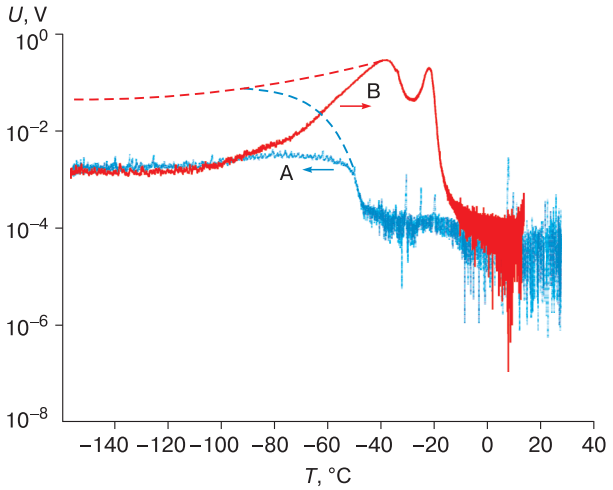

Fig. 2. The results of measuring the mean value of the noise amplitude U of a wetted SBA-15 sample at the output of the measuring device depending on temperature T of the material at cooling (A) and heating (B).

Dashed lines stand for the values of noise voltage after computing the cell impedance increment.

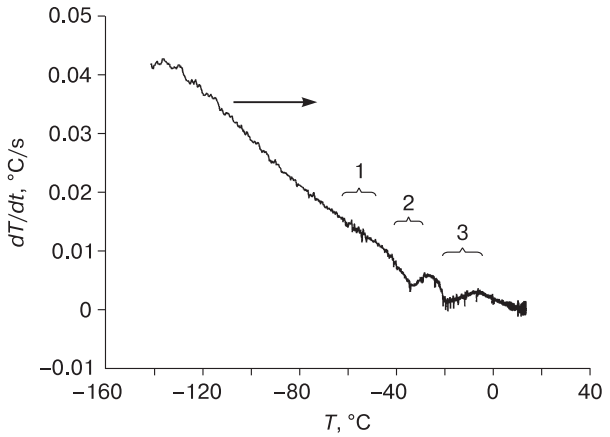

Fig. 3. Dependence of the sample temperature change (dT/dt) at its uniform heating.

1–3 – areas of phase transitions in the medium.

sisted in using broad-band emissions generated by noise generators ($NG_{1,2}$) with a band of ~10 % of average frequency. This allowed us to average signals by frequency and to reduce the number of possible measurement errors when inhomogeneities (discontinuities) were formed, the sizes of which are comparable to the emission wavelength in wetted frozen medium. The same refers to the choice of a sufficiently long waveguide: its length l is much greater than the average emission wavelength λ in the medium ($l \geqslant 10\lambda$). In this sample, spatial averaging of the medium characteristics takes place. The semiconductor-based noise generator NG_1 in the lay-out of the setup (Fig. 1) was used for measuring the emission power losses on passage through the waveguide, and NG_2 was used to determine the reflection index by the power from the flat border of the medium in question in the waveguide. The average signal frequency of the NG was determined by the choice of the detector characteristics and constituted 12.2 GHz, while the width of the frequency band was 1.0 GHz. As a detector, a modulation radiometer was used. The use of attenuators ($ATT_{1,2}$) together with adjustment of the radiometer's sensitivity allowed us to obtain a large dynamic range of the measured signal power values ~50 dB, which is important in case of significant changes in the attenuation of the medium under study when water freezes in it.

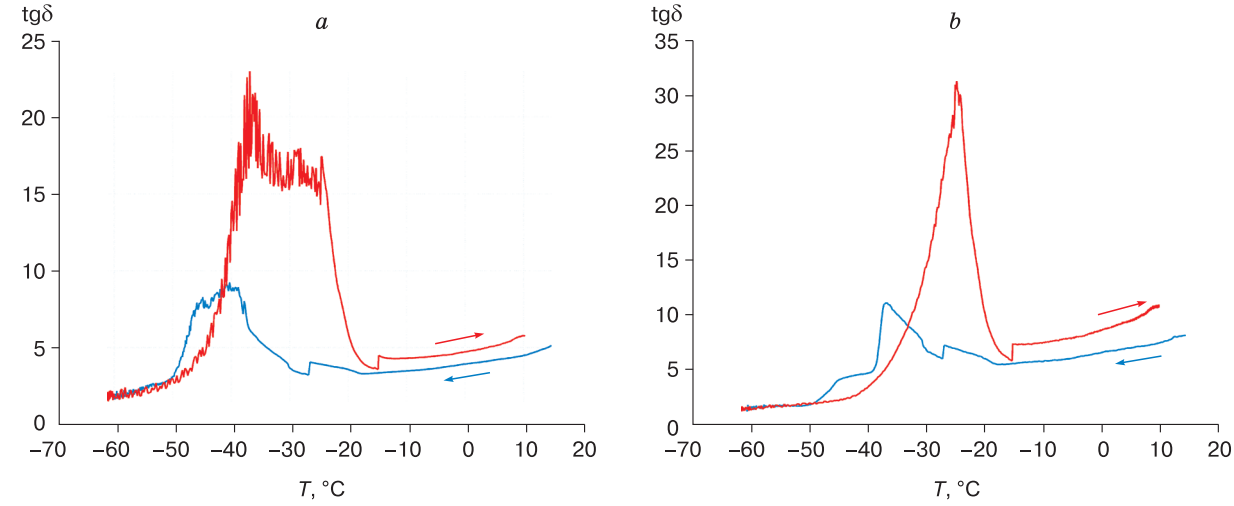

Fig. 4. Dependence of the tangent of the angle of dielectric losses (tg δ) of sample SBA-15 on temperature:

a – frequency 120 Hz; *b* – frequency 1 kHz. The water content of the sample is 40 %.

The measurement results. In the process of the study, we identified the peculiar characteristics of the medium behavior, which were typical of ferroelectric phase transitions: the areas of critical changes in the noise voltage, noise hysteresis and non-uniform change in the thermal properties.

Figs. 2, 3 demonstrate the measurement results of electric noises and of the derivative temperature of the sample by time for SBA-15 with the water content of 70 %, which is close to complete filling of the pore space with water. As it follows from Fig. 2, the cell's noises essentially change, depending on the temperature and the direction of its change; therefore, in order to obtain additional information, we did measurements of dielectric parameters SBA-15 at the frequencies of 120 Hz and 1 kHz. Figure 4 demonstrates the results of measuring the tangent of the angle of dielectric losses at cyclic changes in the temperature of the medium placed in the capacitive cell. Figure 5 shows capacitance measurement results at the frequency of 100 kHz for the same material.

The results of microwave emission measurements are shown in Fig. 6. They were made for silica gel with the water content of 3.5 %. Fig. 6, *a* shows the results of measuring attenuation (L) of emission in the waveguide at the frequency of 12.2 GHz depending on temperature. Attenuation may be represented by the expression

$$L = 10 \lg (P_0/P),$$

where P_0 is power at the input flange of the waveguide containing a silica gel sample; P is the signal power at the waveguide's output to the medium.

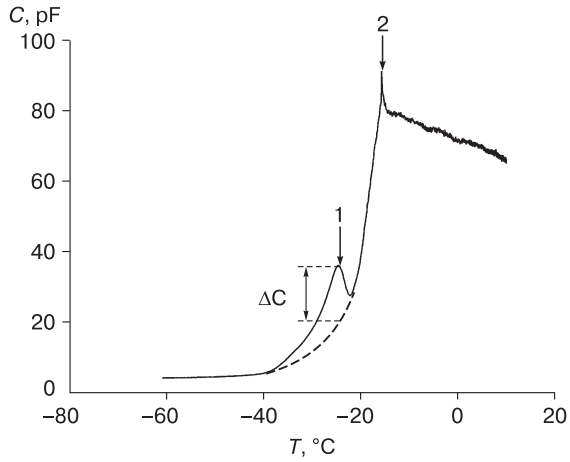

Fig. 5. The temperature dependence of electric capacitance C of the cell filled with wetted SBA-15, in the process of medium heating at the frequency 100 kHz.

1, 2 – capacitance extremes (2 – capacitance jump in the percolation point near −15 °C); the high value of the cell capacitance at temperatures higher than the percolation point is attributed to electrode effects. ΔC – capacitance increment of unknown nature near −25 °C.

Fig. 6, *b* shows the dependence of the emission reflection factor by power from the medium border in the waveguide, determined by the formula:

$$R = P_{refl}/P_0,$$

where P_{refl} is the power of emission reflected from the input flange.

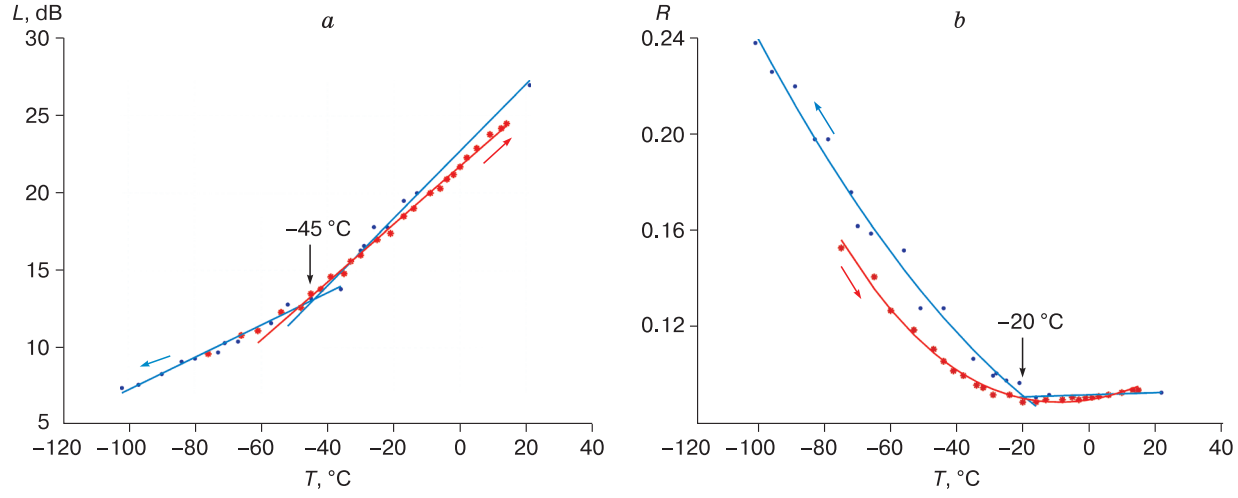

Fig. 6. Results of measuring loss L in microwave emission in a waveguide filled with silica gel Acros with pore size 6 nm (*a*) and plots of the reflection factor R by power (*b*) in relation to temperature.

The arrows near the plots indicate the directions of the medium temperature change; the temperatures of the changes in the plot slant are indicated. The water content is 3.5 %.

The various measurements allowed us to make reliable conclusions regarding the transformations that took place in the wetted nanoporous medium at cyclic change of temperatures.

DISCUSSION OF RESULTS

The results shown in the figures are the following.

Measurements of electric noises. Figure 2 demonstrates essential increment of noise of the cooled SBA-15 in the section of material heating, especially at the temperatures from –60 to –18 °C. The hysteresis of the noise voltage range in the cyclic cooling-heating process is steep. Such behavior is characteristic of ferroelectric materials [*Strukov and Levanyuk, 1983*]. The difference between the noise voltage ranges reaches three orders of magnitude in the indicated range of temperatures.

The derivative dT/dt helps the first-order phase transitions to be revealed. Figure 3 shows its plot for heating of a SBA-15 sample. Three phase transitions are noted: 1 – in the range of temperatures –60...–50 °C (poorly expressed); 2 – in the range of temperatures –40...–28 °C (clearly expressed, with heat absorption); 3 – the phase transition in the indicated range of temperatures from –22 to –10 °C. The first transition corresponds to 2-nm pores and a small amount of water in their volume. When ice melted in those pores, a certain increase in the intensity of electric fluctuations was observed. Two subsequent phase transitions seem to have resulted in two strongly expressed extreme values of noise voltage close in terms of temperatures.

In [*Bordonskiy and Orlov, 2014*], this feature was interpreted as appearance of through conductivity (percolation) near –15 °C, which was evaluated by the change of capacitance related to temperature (Fig. 5). However, the percolation effect may be evaluated by the value of the tangent of the angle of dielectric losses, which in this case should be close to unity [*Emets, 2002; Bordonskiy et al., 2006*]. It follows from Fig. 4 that tg δ at the frequencies 120 Hz and 1 kHz reaches 20–30, which does not correspond to the percolation effect. The high values of tg δ may be explained by the high losses in the medium (essential increase of ε″ compared to ε′), with the extreme at the frequency 1 kHz being narrow and corresponding to –24 °C, where maximum susceptibility (i.e., instability of the domain structure of the medium) seems to have taken place. The noise dropped 1000 times in the range of temperatures from –22 to –10 °C.

It seems to us that these results may be interpreted as melting of the mixture of the ferroelectric ice and paraelectric ice.

Low-frequency dielectric measurements. Additional information may be obtained by considering plots for the tangent of the angle of dielectric losses at cyclic temperature change. At cooling, maximum tg δ was observed at temperatures from –30 to –48 °C, with the extreme value at the frequency 120 Hz being extended in the range of ~15 °C and shifted to lower temperatures. At medium heating, as well as in the preceding process, tg δ had a contrasting extreme value at the frequency 1 kHz, which was centered around –24 °C. The value of tg δ at heating the medium was three times higher than at cooling. This may be explained by the fact that, as ferroelectric ice decomposes, electromagnetic losses in the medium increase.

Microwave measurements. The microwave measurements revealed two specific points in the plots of dependences of electromagnetic losses and the reflection factor got wetted silica gel Acros (Fig. 6). These are the temperatures –45 and –20 °C. The first temperature value corresponds to a change in the slant of the radiation loss plot for radiation that has passed through the waveguide with the medium under study. Plot $L(T)$ is represented on a semilogarithmic scale in Fig. 6, *a*. The other value –20 °C corresponds to the beginning of the sharp uniformly rising reflection factor by power (R) from the flat boundary of the medium in the waveguide, which was observed up to –90 °C of limit temperature for those measurements.

Changing of the slant of plots in Fig. 6, *a* near –45 °C may be related to a change in the attenuation factor α, determined from the relation [*Strukov and Levanyuk, 1983*]

$$P = P_0 \exp(-\alpha Z),$$

where Z is the distance passed by a flat electromagnetic wave; $\alpha = \ln(P_0/P)/Z$.

The attenuation factor for power for homogeneous medium without scatter is related to ε′ and ε″ by the following equation [*Bohren and Huffman, 1986*]:

$$\alpha = 4\pi k/\lambda,$$

where k is the imaginary term of the refraction factor: $k = \{0.5[(\varepsilon'^2 + \varepsilon''^2)^{1/2} - \varepsilon']\}^{1/2}$.

It is likely that, if the derivative $d\alpha/dT$ has a steep rise at –45 °C (i.e., the slant of plot lg (P_0/P) changes), this indicates sharp change of the medium characteristics, for example, at phase transition.

It is known that at atmospheric pressure the temperature –45 °C corresponds to the λ-point (the point of divergence), at which a number of physical parameters of water (heat capacity at constant pressure, isothermal compressibility, etc.) undergo a drastic change [*Mishima, 2010; Holten et al., 2012*]. It is assumed in some papers that the λ-point corresponds to the so-called Widom line, starting from the hypothetical second critical point of water, existing at $T = -53$ °C and at pressure $P \approx 30$ MPA [*Anisimov, 2012*]. However, studying the behavior of media near the λ-point is beyond the scope of this work.

It is to be noted that the special value of the temperature –20 °C determined from the plots of Fig. 6, *b* did not appear in the plot $L(T)$ in Fig. 6, *a*. However, at this point the reflection index is shown to have had a quality change – the angle of deflection of the tangent at T decrease. This indicates that dependence ε'' on temperature (electromagnetic losses on temperature) did not practically change but dependence ε' of the medium in two temperature ranges divided by the value of –20 °C changed significantly. If $\varepsilon' >> \varepsilon''$, the formula for the reflection index by power looks as follows [*Bohren and Huffman, 1986*]

$$R = \left[\left(\sqrt{\varepsilon'} - 1\right)\Big/\left(\sqrt{\varepsilon'} + 1\right)\right]^2.$$

We may assume that at the temperature below –20 °C, phase transition took place in liquid water with gradual increment of the mass in the new phase. What seems to be uncommon in the plots of Fig. 6, *b* is the uniform and significant increase of the reflection index from 0.04 to 0.24, suggesting the special properties of water and ice in the silica gel pores. As the microwave radiation values of ε' of different modifications of ice are close, we may assume the appearance of fine highly conductive films at the boundary ice 0–ice Ih. Such an effect was discovered in [*Korobeynikov et al., 2002, 2005*], it is manifested at the boundary between two dielectrics with a large difference in the static dielectric permittivity ε_s. It is natural to expect its manifestation for the case of contact between ferroelectric and paraelectric ice. At the same time, the growth in the wetness of silica gel Acros to 12.1 % (water content) resulted in the disappearance of this anomaly of the reflection factor. This suggests complex dynamics of the microwave characteristics of water depending on the degree of filling the pore space. It seems that in this case the process of water freezing with ice Ih formed began at the temperatures above the temperature of formation of ice 0 (at greater moisture content, the temperature of phase transition rises [*Schreiber et al., 2001*]). In any case, it was important that a special temperature discriminating the character of the medium behavior was revealed.

Possible observed modifications of ice. All the results shown above and obtained using different techniques may be related to the emergence of nanoscale materials in supercooled water – the ferroelectric phase. We may assume this to be ice XI, formed from ice Ih or ice Ic during ordering of protons. This is a long process, it may last thousands of years, but it gets accelerated when ice is doped, for example, with salt KNO_3 [*Chaplin, 2016*]. It is likely that in the pore space, where supercooled water may exist, and where the phase transition itself is extended over a significant range of temperatures, ice XI may form much faster. Here, however, there are restrictions determined by the shape of pores. In long filament-like pores of such materials as SBA-15 or MCM-41, formation of the ferroelectric phase is easy due to the reduction of the scattering fields at the ends of domains in the filaments. Hence, it is reasonable to search for ferroelectric ice in such media. Indeed, the experiments on measuring electric noise in the SBA-15 samples provided a positive result, whereas for other media (silica gels KSKG and Acros, with pore diameter 6–8 nm, close to spherical shapes) such enhancement of noise has not been detected. At the same time, in the experiments with noise, no ice doping took place: water came to pores during its condensation from saturated water vapor in the dessicator. At the same time, the experiments with silica gels demonstrated their unusual microwave properties, which got manifested during cooling of the media below –20 °C. In the microwave experiment, there are no grounds to expect emergence of ice XI, as in the phase diagram it is rather far from this temperature, the more so as the cooling process started with positive temperatures.

The new data on another modification of the ferroelectric ice, ice 0, the melting point of which is –23 °C [*Quigley et al., 2014; Russo et al., 2014*], explain the results obtained quite well. It is natural to expect that the influence of the wall material will be revealed on water in the pore space; so, there will be variations in the temperatures of formation and melting of ice 0. The performed measurements demonstrate that the unusual electric properties are observed at the temperatures from –20 to –35 °C. Here it is necessary to consider the complex processes of interaction between two types of ice, ice Ih and ice 0, which have not been investigated yet. It is to be pointed out that in [*Menshikov and Fedichev, 2011*], the possibility of transition of supercooled water from the paraelectric state to the ferroelectric state at the temperature within the range of –37...–45 °C was theoretically predicted. This state was discovered in the experiment was nanoporous silicate MCM-41 with such pore sizes, for which liquid water does not freeze until –37...–45 °C [*Fedichev et al., 2011*]; in the experiment, the method of dielectric spectroscopy was used. However, these results are related to the properties of liquid supercooled water. Previous experiments on discovery the ferroelectric properties of ice were mentioned in the monograph [*Bogorodskiy and Gavrilo, 1980*]; however, they were not validated in the subsequent experiments. Perhaps, those were observations of ferroelectric ice 0, although supercooled temperature below –23 °C is required for it to be formed, which fact the authors of the previously performed studies seem to have missed.

CONCLUSIONS

1. The properties of frozen dispersed media discovered in the experiments held, as well as the data

provided by other researchers, are explained by the emergence of a ferroelectric state in moist media, i.e., formation and decomposition of an electric domain structure. These structures are sensitive both to external electric fields and to other physical factors (temperature, mechanical impacts, radiation, etc.).

2. Ice 0 detected during the study of phase transition by the molecular dynamic methods is the most probable object emerging during supercooling by dozens of degrees and freezing of water in finely dispersed media [*Quigley et al., 2014; Russo et al., 2014*]. This modification of ice is formed from supercooled water, with its melting point being –23 °C. In the experiment on measuring the tangent of the angle of dielectric losses of material SBA-15 at the frequency 1 kHz, its extreme value was observed near –24 °C during heating of the sample. This extreme value is explained by formation of the given modification of ice from supercooled water below this temperature, which may be obtained mainly in media with nanopores.

3. The properties of ice 0 are practically unknown. There are questions relating to the temperature ranges of its existence, its interaction with common ice (formation of water films in the boundary layers and on the surface of solid particles, the particular features of their electric characteristics, etc.). Having a chemical potential which is different from that of ice Ih, ice 0 may display increased chemical activity, especially at cyclic changes of temperature near the interval of temperatures of its melting and formation (presumably from –20 to –35 °C).

4. The question of existence of ice XI in terrestrial conditions (at atmospheric pressure and the temperatures ranging from 0 to –90 °C) remains open. It is quite likely that it may form in filament-like pores having a diameter of unities of nanometers, in which the scatter fields of the domain structure are minimized, as well as in the presence of additives. This question requires further study.

References

Anisimov, M.A., 2012. Cold and supercooled water as an unusual supercritical fluid, in: Supercritical Fluids: Theory and Practice 7 (2), 19–37.

Arakawa, M., Kagi, H., Fernandez-Baca, J.A., et al., 2011. The existence of memory effect on hydrogen ordering in ice: The effect makes ice attractive. Geophys. Res. Lett. 38 (16), L16101-5.

Bogorodskiy, V.V., Gavrilo, V.P., 1980. Ice. Its Physical Properties. Modern Glaciology Methods. Gidrometeoizdat, Leningrad, 384 pp. (in Russian)

Bohren, C., Huffman, D., 1986. Absorption and Scattering of Light by Small Particles, Mir, Moscow, 664 pp. (in Russian)

Bordonskiy, G.S., Krylov, S.D., 2012. Structural transformations of supercooled water in nanopores according to data on absorption of microwave radiation. Zhurnal Fizicheskoy Khimii 86 (11), 1806–1812.

Bordonskiy, G.S., Orlov, A.O., 2014. The study of ferroelectric phase transitions of water in nanopore silicates at joint electrical background and calorimetric measurements. Fizika Tverdogo Tela 56 (8), 1575–1582.

Bordonskiy, G.S., Orlov, A.O., Filippova, T.G., 2006. The temperature dependence of electrical parameters of frozen sand at low frequencies. Radiotekhnika i Electronika 51 (3), 314–319.

Castrillon, S.R.-V., Giovambattista, N., Arsay, I.A., Debenedetti, P.G., 2009. Evolution from surface-influenced to bulk-like dynamics in nanoscopically confined water. J. Phys. Chemistry B, vol. 113, 7973–7976.

Chaplin, M. Ice phases [Electronic Resource]. – URL: http://www.lsbu.ac.uk/water/ice-phases.html (submittal date: 02.09.2016).

Emets, Y.P., 2002. Dispersion of dielectric permittivity of two-component media. Zhurnal Eksperimentalnoy i Teoreticheskoy Fiziki 121 (6), 1339–1351.

Fedichev, P.O., Menshikov, L.I., Bordonskiy, G.S., Orlov, A.O., 2011. Experimental evidence of the ferroelectric nature of the λ-point transition in liquid water. JETP Lett. 94 (5), 401–405.

Fedichev, P.O., Menshikov, L.I., 2012. How does confinement in nano-scale pores change the thermodynamic properties and the nature of phase transitions of water? Preprint arXiv: 1206.3470 [cond-mat.soft], Cornell Univ., 15 Jan. 2012, 3 p.

Fedichev, P.O., Menshikov, L.I., 2013. Application of the two-liquid model for the interpretation of the observed electrophysical properties of supercooled water in nanopores. JETP Lett. 97 (4), 214–219.

Fortes, A.D., Wood, I.G., Grigoriev, D., et al., 2004. No evidence for large-scale proton ordering in Antarctic ice from powder neutron diffraction. J. Chemical Phys. 120, 11376–11379.

Fukazawa, H., Hoshikawa, A., Ishii, Y., et al., 2006. Existence of ferroelectric ice in the universe. Astrophys. J. 652 (1), L57–L60.

Fukazawa, H., Mae, S., Ikeda, S., Watanabe, O., 1998. Proton ordering in Antarctic ice observed by Raman and neutron scattering. Chemical Phys. Lett. 294, 554–558.

Holten, V., Bertrand, C.E., Anisimov, M.A., Sengers, J.V., 2012. Thermodynamics of supercooled water. J. Chemical Phys. 136, p. 094507/23.

Jazdzewska, M., Śliwinska-Bartkowiak, M.M., Beskrovnyy, A.I., et al., 2011. Novel ice structures in carbon nanopores: pressure enhancement effect of confinement. Phys. Chemistry Chem. Physics 13 (19), 9008–9013.

Kirov, M.V., 1996. Proton ordering of hexagonal ice. Zhurnal Strukturnoy Khimii 37 (6), 1089–1098.

Korobeynikov, S.M., Drozhzhin, A.P., Furin, G.G., et al., 2002. Surface conductivity in liquid-solid interface due to image force, in: Proc. of 2002 IEEE 14th Intern. Conf. on Dielectric Liquids (ICDL 2002), Graz (Austria), July 7–12, 2002, Piscataway, NJ: IEEE, pp. 270–273.

Korobeynikov, S.M., Melekhov, A.V., Soloveitchik, Yu.G., et al., 2005. Surface conductivity at the interface between ceramics and transformer oil. J. Physics D: Appl. Phys. 38 (6), 915–921.

Limmer, D.T., Chandler, D., 2012. Phase diagram of supercooled water confined to hydrophilic nanopores. J. Chemical Phys. 137, p. 044509/11.

Menshikov, L.I., Fedichev, P.O., 2011. Possible existence of the ferroelectric state of supercooled water. Zhurnal Fizicheskoy Khimii 85 (5), 996–998.

Mishima, O., 2010. Volume of supercooled water under pressure and the liquid-liquid critical point. J. Chemical Phys. 133, p. 144503/6.

Musevic, I., Kityk, A., Skarabot, M., Blinc, R., 1997. Polarization noise in a ferroelectric liquid crystal. Physical Rev. Lett. 79 (6), 1062–1065.

Pan, D., Liu, L.M., Tribello, G.A., et al., 2008. Surface energy and surface proton order of ice Ih. Physical Rev. Lett. 101 (15), p. 155703/4.

Quigley, D., Alfè, D., Slater, B., 2014. Communication: On the stability of ice 0, ice I, and Ih. J. Chemical Phys. 141, p. 161102.

Rosenfeld, D., Woodley, W.L., 2000. Deep convective clouds with sustained supercooled liquid water down to –37.5 °C. Nature, vol. 405, 440–442.

Russo, J., Romano, F., Tanaka, H., 2014. New metastable form of ice and its role in the homogeneous crystallization of water. Nature Materials, vol. 13, 733–793.

Schreiber, A., Kotelsen, I., Findenegy, G.H., 2001. Melting and freezing of water in ordered mesoporous silica materials. Phys. Chemistry Chem. Physics, vol. 3, 1185–1195.

Sliwinska-Bartkowiak, M., Jazdzewska, M., Huang, L.L., Gubbins, K.E., 2008. Melting behavior of water in cylindrical pores: carbon nanotubes and silica glasses. Phys. Chemistry Chem. Physics 10 (32), 4909–4919.

Strukov, B.A., Levanyuk, A.P., 1983. Physical Foundations of Ferroelectric Phenomena in Crystals. Nauka, Moscow, 240 pp. (in Russian)

Stukova, E.V., Baryshnikov, S.B., Shatskaya, Yu.A., et al., 2012. The study of the ferroelectric phase transition in nanoscale sodium nitrite by the method of thermal noise. Phys. Procedia, vol. 23, 77–80.

Su, X., Lianos, L., Shen, Y.R., Somorjai, G.A., 1998. Surface-induced ferroelectric Ice on Pt (111). Physical Rev. Lett. 80 (7), 1533–1536.

Zhao, H.X., Kong, X.J., Li, H., et al., 2011. Transition from one-dimensional water to ferroelectric ice within a supramolecular architecture. Proc. of the National Academy of Sciences, 108 (9), 3481–3486.

Received September 9, 2016